

The Effect of Local Atmospheric Circulations on Daytime Carbon Dioxide Flux Measurements over a *Pinus elliottii* Canopy

H. W. LOESCHER

Department of Forest Science, Oregon State University, Corvallis, Oregon

G. STARR AND T. A. MARTIN

School of Forest Resources and Conservation, University of Florida, Gainesville, Florida

M. BINFORD

Department of Geography, University of Florida, Gainesville, Florida

H. L. GHOLZ

Division of Environmental Biology, National Science Foundation, Arlington, Virginia

(Manuscript received 12 January 2005, in final form 14 October 2005)

ABSTRACT

The daytime net ecosystem exchange of CO₂ (NEE) was measured in an even-aged slash pine plantation in northern Florida from 1999 to 2001 using the eddy covariance technique. In August 2000, two clear-cuts were formed approximately 1 km west of the study site. A statistical approach was used to determine whether the clear-cuts induced changes in CO₂ concentration, wind direction, horizontal and vertical wind speeds, and temperature, as measured by instruments above the plantation canopy and, in turn, whether any such changes affected daytime NEE. The NEE estimates were first transformed so that mean responses to incident radiation and vapor pressure deficit were removed using empirically derived functions for each 30-min period. Prior to the clear-cuts, there were significant interactive effects of CO₂ concentration and some wind statistics on NEE at the tower when wind was flowing from the direction of the future clear-cuts. Even in this relatively homogenous forest, with flat topography, the CO₂ source strength differed with wind direction prior to the clear-cuts. After the clear-cuts, additional two- and three-way interactive effects became significant during flows from the direction of the clear-cuts. There was also a 16.6% reduction in the integrated measure of daytime NEE over 487 days after the clear-cuts. The results herein suggest that the development of local circulations over the clear-cuts contributed to low-frequency effects on the NEE.

1. Introduction

The surface–atmosphere exchange measured by eddy covariance, plus independent measurements of the change in CO₂ storage below canopy, have been used to provide estimates of net ecosystem exchange of carbon dioxide (NEE) (Black et al. 2000; Greco and Baldocchi 1996; Valentini et al. 1996; Goulden et al. 1996; Running et al. 1999; Pilegaard et al. 2001). Assumptions

underlying the use of this technique include spatial homogeneity in the source area for both the above- and below-canopy environments. Efforts to increase the application of eddy covariance precision and accuracy in NEE estimates are now increasingly focused on measurements in complex and challenging flows, for example, spatial inhomogeneities and advection (e.g., Loescher et al. 2006). Jarvis et al. (1997) and Goulden et al. (1996) first suggested that there may be “missing CO₂” transported from the below-canopy environment associated with cold-air drainage. Since then, advection has been shown to export significant amounts of CO₂ from both below- and above-canopy environments, such as in the old-growth conifer forest studied by M.

Corresponding author address: Henry W. Loescher, Department of Forest Science, College of Forestry, 321 Richardson Hall, Oregon State University, Corvallis, OR 97311.
E-mail: hank.loescher@oregonstate.edu

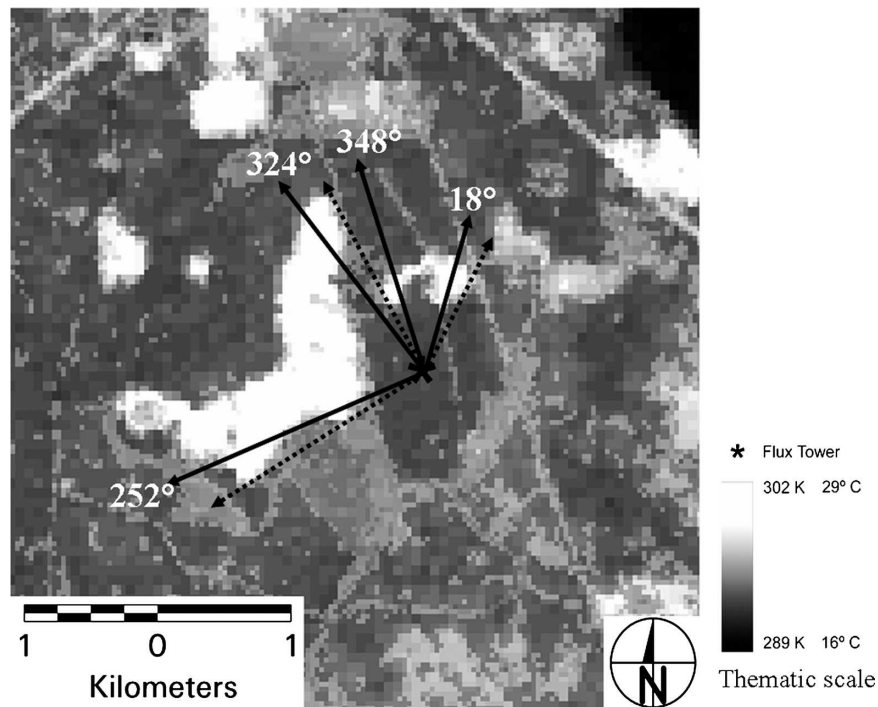


FIG. 1. Effective surface temperatures derived from the ETM+. Dotted arrows indicate the vectors considered to be the boundaries of the clear-cuts. Because the std dev of θ was $\sim \pm 20^\circ$, we functionally defined the categorical variable *cc* (used in ANOVA) as beginning $\pm 12^\circ$ inside the edge of the clear-cut to avoid contamination from edge effects. These vectors are indicated by the solid arrows. Data were from 1055 eastern standard time 20 Jan 2000. The areas intermediate in shading include deciduous wetland forests, roads, and formerly clear-cut areas in various stages of regrowth.

Falk (2004, personal communication) and Paw U et al. (2000). Spatial inhomogeneities, such as clearings (Leclerc et al. 2003), bodies of water (Sun et al. 1998), or sparse vegetation, can significantly increase thermal convection and introduce locally generated circulations, thereby changing mean wind flow and turbulence characteristics and introducing additional uncertainties into NEE estimates (Letzel and Raasch 2003; Kanda et al. 2004). Understanding and subsequently reducing these errors is important because many flux measurement sites are characterized by a complex vegetation structure, complex topography, and/or spatial legacies of land use, thus making advection estimates particularly difficult.

In August of 2000, clear-cut logging of a pine plantation near the midrotation Florida slash pine AmeriFlux site created two large patches of exposed soil and litter with contrasting ecological, energy, and mass exchange attributes (Fig. 1). Use of a footprint model (Schuepp et al. 1990) suggested that the clear-cuts were outside the footprint for $>90\%$ of the cumulative flux at the tower site. However, a tracer (SF_6) experiment during this period suggested otherwise, and it was not

possible to resolve the flux source area when the wind was predominantly from the direction of the larger clear-cut (Leclerc et al. 2003). One possibility was that higher CO_2 concentrations and lower NEE would occur at the tower when air masses from the clear-cuts were horizontally advected after morning heating of the surface (Fig. 2; Leclerc et al. 2003). This explanation is contrary to the assumptions made when applying eddy covariance for any time-averaged estimate—that surface flux characteristics are spatially homogeneous (spatially uniform source and sink strength regardless of the source area). We used a statistical approach to test if changes in wind speed and direction, CO_2 concentrations, and temperature as a result of the clear-cuts could affect mean daytime NEE at the flux tower in the intact forest almost a kilometer away.

2. Methods

a. Study site

This study was conducted at the Florida AmeriFlux site, a closed-canopy, midrotation slash pine (*Pinus elliotii*) plantation located ~ 15 km northeast of Gaines-

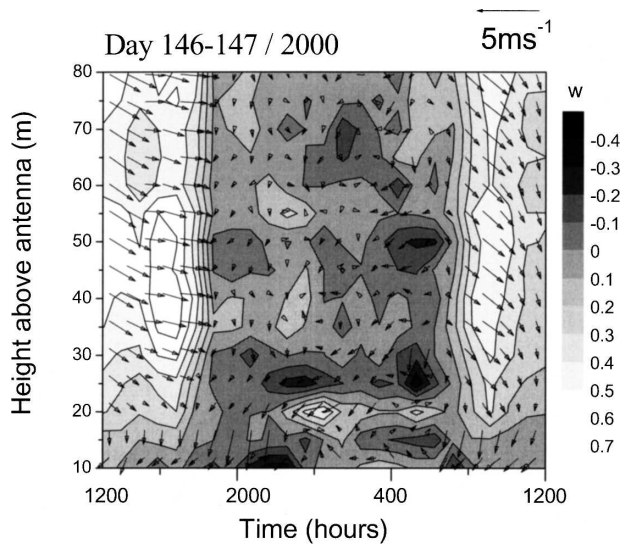


FIG. 2. Hourly averaged horizontal and vertical velocities as a function of height estimated by a minisodar (Boku, Vienna, Austria) in the clear-cut area (see Fig. 1). Shaded contour plot depicts vertical velocities and arrows represent horizontal velocities. The length and direction of the arrows shows the relative magnitude and orientation of the horizontal flows, respectively. Data are from the advent of the clear-cut on day of year (DOY) 146–147. The daytime vertical velocities were typically positive (updrafts), strong, and systematic. [Reprinted from Leclerc et al. (2003) with permission from Elsevier.]

ville, Florida ($29^{\circ}45'9''\text{N}$, $82^{\circ}9'45''\text{W}$; elevation 50 m), referred to as the Donaldson site. The 40-ha study stand was planted in 1990 and was located within a larger matrix (hundreds of hectares) of other slash pine plantations of a similar age (± 3 yr) and structure. The topography was flat. At the time of the study, the mean canopy height was ~ 10 m. The mean monthly air temperatures were 14° and 27°C in January and July, respectively (1955–95), and the mean annual precipitation was 1320 mm, as obtained from the National Climatic Data Center for the Gainesville Regional Airport. A more detailed description of the ecosystem can be found in Clark et al. (2004), Gholz and Clark (2002), and online (see information at http://public.ornl.gov/ameriflux/Site_Info).

The larger clear-cut was created ~ 750 m west of the flux tower and was irregularly shaped, ranging from ~ 450 to 1250 m in length and from 50 to 600 m in width. The smaller clear-cut was ~ 750 m north of the flux tower and was also irregularly shaped (Fig. 1). All of the tree stems were removed, with branches, foliage, and litter left on site. Saw palmetto (*Serenoa repens*) and a small herbaceous layer began to regenerate vegetatively within weeks after the clearing, although much of the soil and litter was directly exposed to solar irradiance. In typical style for the region, the area was

bedded and then planted with *P. elliotii* seedlings during the spring of 2001.

b. Micrometeorology

Fluxes of CO_2 were measured using eddy covariance (Clark et al. 1999, 2004; Moncrieff et al. 1997), consisting of a 3D sonic anemometer (model R3, Gill Instruments, Ltd., Lymington, United Kingdom) and a fast-response closed-path infrared gas analyzer (IRGA; Li-6262, Li-Cor, Inc., Lincoln, Nebraska) mounted on a tower. The tower was located in the 40-ha study area in the *P. elliotii* plantation. Air was drawn continuously from the inlet collocated with the sonic anemometer through ~ 30 m of 0.4-cm inside-diameter tubing to the IRGA. A flow rate of 6.0 L min^{-1} was maintained by an air pump and mass flow controller. Data were collected at a frequency of 10 Hz using a computer and were postprocessed into 30-min averages. Sensor separation was accounted for by determining the correlation coefficient between vertical wind speed and the CO_2 signal for each 30-min period. Two-dimensional coordinate rotation aligned the flow parallel to local streamline for each 30-min period. Rotation angles were within the manufacturer's limits, in part because the canopy had a short aerodynamic roughness and the topography was flat. Time-averaged estimates of vertical velocities and scalar fluxes calculated with 2D rotation likely do not differ significantly from those estimated using planar fit (cf. Wilczak et al. 2001) when measured over such a relatively ideal site for surface flux measurements as that observed at the Donaldson site (i.e., topographically flat and homogeneous canopies with short roughness lengths; T. Meyers and L. Mahrt 2005, personal communication). The alignment of the R3 anemometer was checked (at least) monthly, and when a repair was needed, a replacement R3 anemometer was realigned to plumb. The R3 was mounted at 16 m in 1999, and was moved each subsequent January to maintain 6-m distance between the anemometer and canopy height. The sonic anemometers used in this study were factory calibrated to assure the accuracy and precision of all of the wind velocities and sonic temperatures [see Loescher et al. (2005a) and Gash and Dolman (2003) for evaluation].

Fast-response horizontal and vertical wind speeds U and w , respectively, and sonic temperature T_s (cf. Loescher et al. 2005a; Kaimal and Gaynor 1991) were measured with the R3. Relative humidity (ES-110, Omnidata, Inc., Ogden, Utah) and air temperature T_a (CS500, Campbell Scientific, Inc., Logan, Utah) were measured in a radiation shield at the same height as the sonic anemometer with a datalogger (model CR10X, Campbell Scientific, Inc.) until October 2000. After

that a Vaisala HMP45C temperature/relative humidity sensor was used instead of the ES-110 and CS500. Reliable data from the ES-110 were not collected during September–December 1999. Air temperature was used to calculate saturation vapor pressure e_s with the equations presented in Buck (1981). Ambient vapor pressure e_a was obtained by multiplying by relative humidity and e_s , and vapor pressure deficit (VPD) calculated as the difference between e_a and e_s . A tipping-bucket rain gauge (model TE-525-L, Texas Electronics, Inc., Dallas, Texas) and an incident radiation sensor (Φ ; Li 190sx, Li-Cor, Inc.) were mounted at the same height as, and near to, the sonic anemometer. Soil temperatures were measured from January 1999 through June 2001 with three sensors (model 108-L, Campbell Scientific, Inc.) at 10-cm depth, and were averaged into one 30-min average. There was 100% data coverage for the meteorological variables, except where noted, and there were less eddy covariance data collected before the clear-cuts than afterward, with 2810 and 9117 30-min daytime averages, respectively.

Monthly Palmer drought severity index (PDSI) values for north Florida over the last century were used to characterize the water availability at spatial scales larger than our immediate flux footprint. Data were from 1895 to 2004 and can be found online (available at <ftp://ftp.ncdc.noaa.gov/pub/data/cirs/>). The index is unitless, with long-term average values ranging from 0.49 to -0.49 , and with increasingly negative values corresponding to drought. Extreme drought conditions are classified as < -4.0 . Complete descriptions of the equations used to estimate the PDSI can be found in Palmer (1965), Alley (1984), and Karl and Knight (1985).

Pinus holds two cohorts of needles during the growing season and one cohort after November and throughout the winter. The ratio of data collected with one to two cohorts was essentially equal in the datasets from before and after the clear-cut, 0.56 and 0.57, respectively.

Losses in CO_2 fluxes arising from the nonideal frequency response of the IRGA, frequency attenuation by the tubing, and errors in sensor separation were accounted for following the transfer function procedure of Moore (1986) and Moncrieff et al. (1997). Protocols for accuracy, precision, and quality control and assurance were used as defined by the AmeriFlux Science Plan (http://public.ornl.gov/ameriflux/about-strategic_plan.shtml). A negative NEE denotes the uptake of carbon by the plantation. Flux data for this study were collected from 1 January 1999 through 31 December 2001.

We used ogive analysis (the integration of cospectra

across longer time intervals) to examine such impacts from 30 min to 2 h (e.g., Berger et al. 2001):

$$\text{Og}_{w,x}(f_0) = \int_{-\infty}^{f_0} \text{Co}_{w,x}(f), \quad (1)$$

where Og are the ogives ($\mu\text{mol CO}_2 \text{ mol}^{-1} \text{ s}^{-1}$) across the integrated frequency f for each sampling period, and Co is the cospectra of w and CO_2 . For each sampling period, each ogive was estimated with averaged quantities over its entire respective time period; for example, block averages and the 2D rotations for a 1-h sampling period were calculated using all the high-frequency data of that particular time period.

c. Normalization of NEE

NEE integrates the interactions between biotic attributes and changing environmental conditions. In this system, Φ and VPD are likely the major environmental determinants of daytime NEE (Teskey et al. 1994; Clark et al. 2004; T. Martin and G. Starr 2005, unpublished manuscript). To minimize the confounding influences of environmental (Φ and VPD) differences pre- and post-clear-cut, we calculated a normalized NEE variable termed NEE_{max} , which reflected the value of NEE for any particular half-hour corrected for reductions resulting from nonoptimum VPD or Φ conditions.

NEE_{max} was calculated using a linear detrending approach similar to that found in Martin et al. (1997) and Wright et al. (1996). First, data were grouped into 2-month periods to capture seasonal variation. Daytime NEE data within each period were normalized to a 0–1 scale by dividing each half-hourly NEE value by the minimum (most negative) NEE value within the 2-month period ($\text{NEE}_{\text{norm-1}}$). When the $\text{NEE}_{\text{norm-1}}$ data were plotted against VPD (in 0.1-kPa bins), the data could be defined by two linear lines as shown in Fig. 3a. Half-hourly measurements with VPD greater than the inflection point at b on Fig. 3a were assumed to be reduced by VPD, and were adjusted to lie along the trajectory ab. This new estimate was then converted back into units of micromoles of CO_2 per meter squared per second and normalized (once again) by the minimum (most negative) value producing $\text{NEE}_{\text{norm-2}}$, which represented the normalized value of NEE, with any effects of VPD adjusted out.

Values of $\text{NEE}_{\text{norm-2}}$ were then plotted against incident radiation, and values in the light-limited region of the scatterplot (line bc in Fig. 3c) were similarly adjusted to remove the limiting effects of radiation. The final resulting value, after transforming back to the original units, was termed NEE_{max} , and reflected the

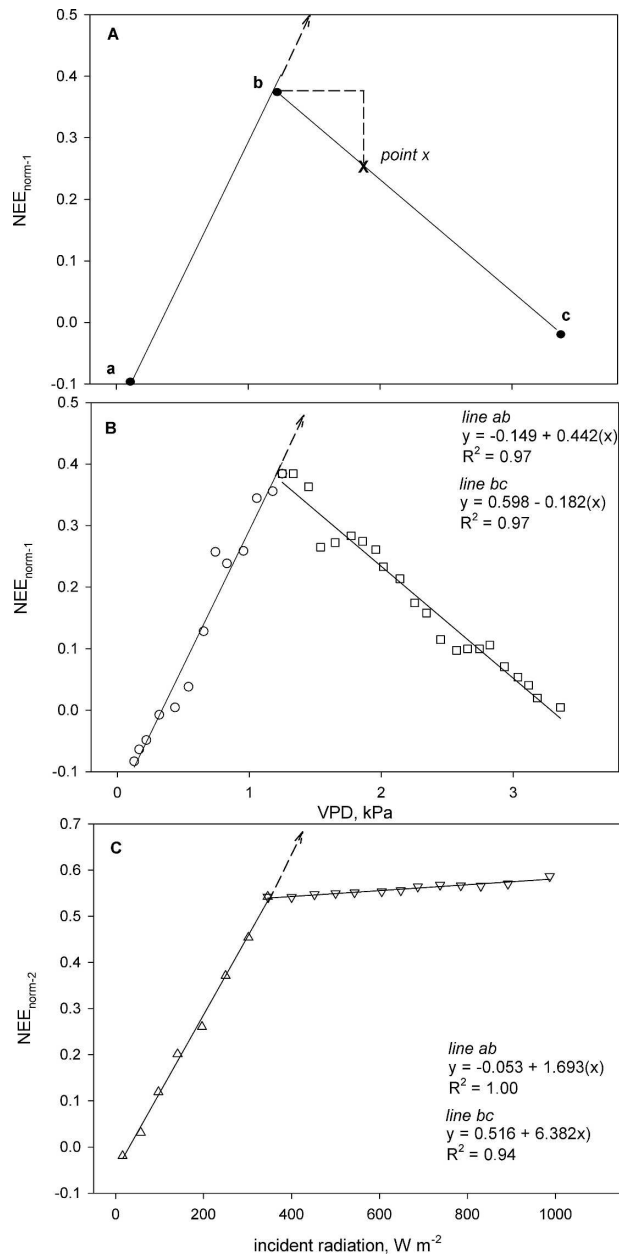


FIG. 3. Determination of daytime NEE that is not limited by both VPD and incident radiation: (a) a conceptual graph depicting the relationship between NEE_{norm-1} and VPD with line ab being conditions where VPD was nonlimiting and line bc being conditions where VPD became limiting; (b) an example of the relationship between NEE_{norm-1} and VPD using data collected from May–Jun 2001 used to determine NEE_{norm-2} [the standard error (SE) for the measured NEE_{norm-1} was typically $<0.07 \mu mol m^{-2} s^{-1}$, and <0.012 kPa for VPD within each data bin]; and (c) an example of the relationship between NEE_{norm-2} and incident radiation using data collected Mar–Apr 2001. Empirical data were from the Donaldson tract, a midrotation-age slash pine stand in Gainesville, FL. NEE_{norm-2} estimates were averaged in $25 W m^{-2}$ bins.

TABLE 1. The mean daily rate of precipitation (mm) based on first-order regression over the Donaldson site. Within-year intervals were determined to separate the summer convective storm activity from other rain events. Rates within a DOY interval were not significantly different. The data shown are slope ± 1 SD, R^2 . Each interval for each year was significant at the $\alpha = 0.05$ level and a $p < 0.0001$.

DOY interval	1999	2000	2001
1–151	1.24 \pm 0.84, 0.88	1.30 \pm 0.60, 0.94	2.25 \pm 1.30, 0.91
152–273	3.87 \pm 0.89, 0.98	4.35 \pm 1.55, 0.96	6.23 \pm 1.77, 0.98
274–365*	1.24 \pm 0.44, 0.94	0.76 \pm 0.41, 0.87	0.79 \pm 0.48, 0.84

* DOY interval for 2000 was 273–366.

measured value of NEE for any particular half-hour, with any reductions resulting from high VPD or Φ adjusted out (see also Jarvis 1976; Livingston and Black 1987). NEE_{max} was used as the dependent variable in a general linear, mixed-effects model [analysis of variance (ANOVA)] to determine the effects of local circulations on the daytime ecosystem exchanges of carbon. Carbon dioxide, wind direction θ , U , T_a , and w were considered as independent and random variables, and a fixed, categorical variable *cc* was used to identify whether flows came from the direction of either clear-cut. The definition of this variable was constrained by horizontal winds that only came from within the boundaries of the clear-cuts. The standard deviation of wind direction θ was $\sim \pm 20^\circ$. The boundaries were defined, in turn, as beginning 12° inside the clear-cuts from the edge of the forest to avoid edge contamination (Fig. 1). This is 2° beyond $1/2$ of the standard deviation (SD) of θ . For all statistical analyses S-plus (version 6.2, MathSoft, Inc., Cambridge, Massachusetts) was used. Wind roses were constructed by bin averaging the wind direction data across 20° at 10° intervals.

d. Supporting datasets

1) MAPPING AND SURFACE TEMPERATURE ESTIMATES

Because we did not have the clear-cuts instrumented, we calculated an effective surface temperature using an image from the Landsat Enhanced Thematic Mapper+ (ETM+) scene [Worldwide Reference System II path 17, row 39; acquisition time of 1554:00 UTC (1054:00 local time) 2 January 2000]. At-satellite temperature was first calculated from band 6 data by converting the 8-bit ETM+ digital numbers to spectral radiance with the gain and bias values given in the scene's metadata file, then calculating effective at-satellite temperature (units: K) using the thermal band calibration constants

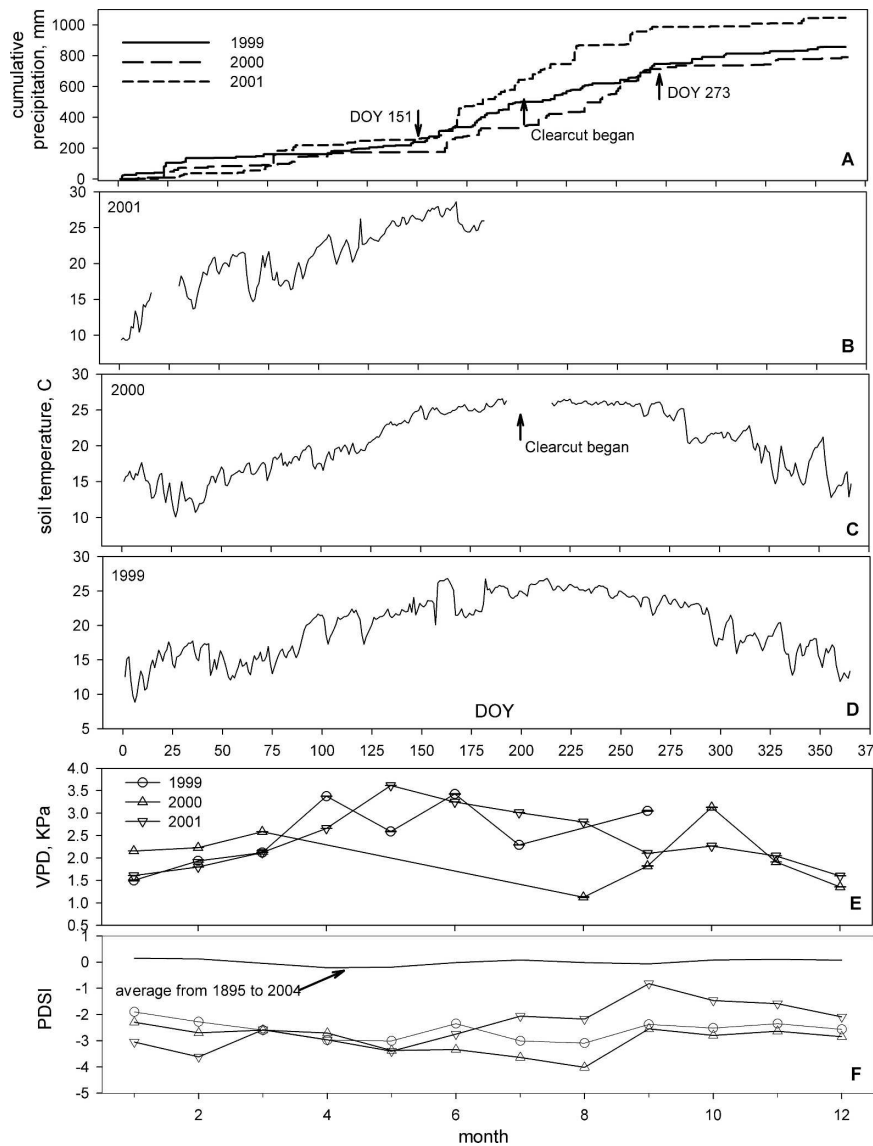


FIG. 4. (a) Cumulative precipitation, (b)–(d) soil temperatures, and (e) VPD estimates from the Donaldson tract tower site. Data from (a)–(d) were 30-min averages, and data from (e) were maximum VPD values at 1530 LT. (f) The Palmer drought severity index. Annual precipitation depth was 857, 791, and 1047 mm during 1999, 2000, and 2001, respectively. The SD for the VPD estimates collected within each month at 1530 LT ranged from 0.24 to 0.85. The SD for the PDSI were $\leq \pm 2.0$ within each month in the long-term average.

and equation given in the *Landsat-7 Science Data User's Handbook* (available online at http://ltpwww.gsfc.nasa.gov/IAS/handbook/handbook_htmls/chapter11/chapter11.html). This calculation assumes 100% black-body emissivity ϵ from all land covers, but emissivity, and therefore calculated surface temperature, varies by land cover (Oke 1978), so the following different ϵ values were assigned to six different land covers based on Synder et al. (1998): water = 0.95, mature pine forest = 0.98, mature hardwood forest = 0.98, midrotational

pine forest = 0.97, young pine forest = 0.96, and clear-cut and herbaceous layer = 0.95. In this case, no atmospheric correction was necessary to account for the scattering and absorption of radiation by gases and aerosols through the atmospheric profile (Song et al. 2001).

2) BUOYANCY FLUX ESTIMATES

The buoyancy flux $\overline{w'T'_s}$ (prime denotes turbulent fluctuations from a time-averaged mean, and the over-

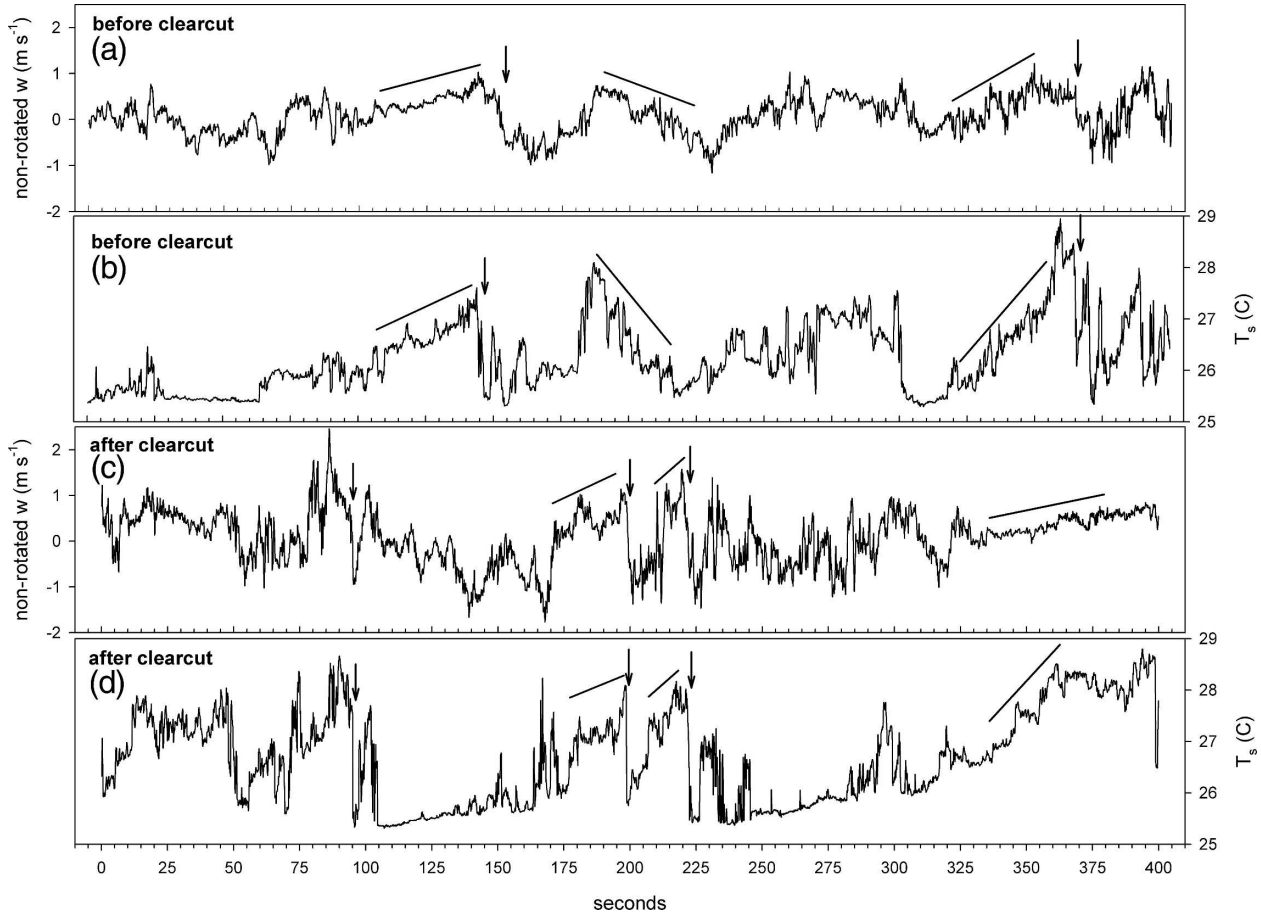


FIG. 5. The 10-Hz time series of nonrotated w and T_s measured before and after the clear-cut from the Donaldson site. Data in graphs were from (a), (b) before and (c), (d) after the clear-cut collected at 0900:00 LT 22 May 1999 and 2001, respectively. Drawn diagonal lines indicate some coherent structures (i.e., ramps) present in both the w and T_s time series. For these two 30-min sampling periods, U , nonrotated w , air temperature, incident radiation, and friction velocity were similar: 1.55 and 1.50 m s^{-1} , -0.06 and 0.04 m s^{-1} , 23.9° and 27.7°C, 439 and 500 W m^{-2} , and 0.40 and 0.42 m s^{-1} , respectively.

bar denotes the estimate as a 30-min average; cf. Loeschler et al. 2005a,b) is likely less sensitive to changes in CO_2 source strength, but is sensitive to its scalar source area. Using the same 10-Hz time series described above to calculate NEE from the Donaldson site, $\overline{w'T'_s}$ was measured. A 2D rotation was then applied and 30-min estimates were calculated. To determine the effects of local circulations, $\overline{w'T'_s}$ was used as the dependent variable in a general linear mixed-effects model (ANOVA). The same fixed, categorical variable of clear-cut was used, and θ , U , and w were considered as independent and random variables.

3) SECOND TOWER SITE

Some differences in microclimate may not be entirely because of the clear-cuts, but rather to changes in regional-scale climate. Vertical and horizontal wind ve-

locities and sonic temperatures from the Donaldson site were contrasted to those from a second site, the Austin Cary Memorial Forest (ACMF), located ~ 4.5 km southeast from the Donaldson site. In this case, a 3D sonic anemometer (WindMaster Pro, Gill Instruments, Ltd., Lymington, United Kingdom) was mounted on a tower at 32 m. This ecosystem was a closed-canopy, uneven-aged, naturally regenerated stand of mixed slash pine and loblolly pine (*P. taeda* L.) with trees ranging from about 10 to 80 yr of age. Mean canopy height was ~ 22 m. Soils were of the same classification as that found at the Donaldson site.

3. Results

Trends in annual precipitation were similar among the years, with the most rainfall occurring during the

months from June to September, which was due to late-afternoon convective thunderstorm activity (Table 1, Fig. 4a). Annual precipitation over the 3 yr was 35%, 40%, and 20% below the long-term average, respectively. There were no significant differences in soil temperatures among the years, even though soil temperatures during the first 6 months of 2001 appear slightly warmer compared with data from 1999 and 2000 (Figs. 4b–d). Assuming the largest VPD values would occur in midafternoon, there was also no significant difference in monthly VPDs measured at 1530 LT, with SD ranging from 0.24 to 0.85 kPa (Fig. 4e). Drought conditions persisted throughout our measurement period across northern Florida (Fig. 4f).

The sonic anemometer was always mounted ~ 6 m above the canopy height in the well-mixed surface layer, which minimized any roughness effects during daytime hours. Coherent structures in w and T_s were evident in high-frequency time series before and after clear-cuts (i.e., the ramp structures in Fig. 5). For comparison, data from the before and after clear-cut periods showed that T_s , U , and nonrotated w for July 2000 and in 2001 from the ACMF site were not significantly different (Fig. 6).

The mean trend of NEE_{norm-1} was linear and positive when VPD was not limiting, and conversely was linear and negative after VPD became limited for each discrete 2-month period (e.g., Fig. 3b). Slopes and thresholds when VPD became limited were different for each period, slopes and thresholds ranged from -0.01 to -0.19 kPa and from 0.23 to 0.79, respectively. The NEE_{norm-2} was also found to be linear and positive when Φ was not limiting, and Φ became limited for each discrete 2-month period (e.g., Fig. 3c).

Using data prior to the clear-cuts, several interactive effects of environmental variables on NEE_{max} were significant, including some originating from the direction of the clear-cuts (Table 2). There were several significant three-way interactions that included some combination of all of the independent variables (Table 2). The only two-way effect that was significant was $\theta * cc$, where the asterisk (*) denotes a statistical interaction. The only main effect that was significant was θ .

Using only data collected after the clear-cuts, all of the same significant effects were found from the previous ANOVA. Three additional two-way effects became significant, $[CO_2] * U$, $[CO_2] * T_a$, and $[CO_2] * cc$ (Table 2), where the brackets indicate the molar fraction. One additional main effect became significant, T_a .

We assumed that the within-forest sources of CO_2 were the same within the boundaries of the clear-cuts before the harvest to that of the intact forest. Finding

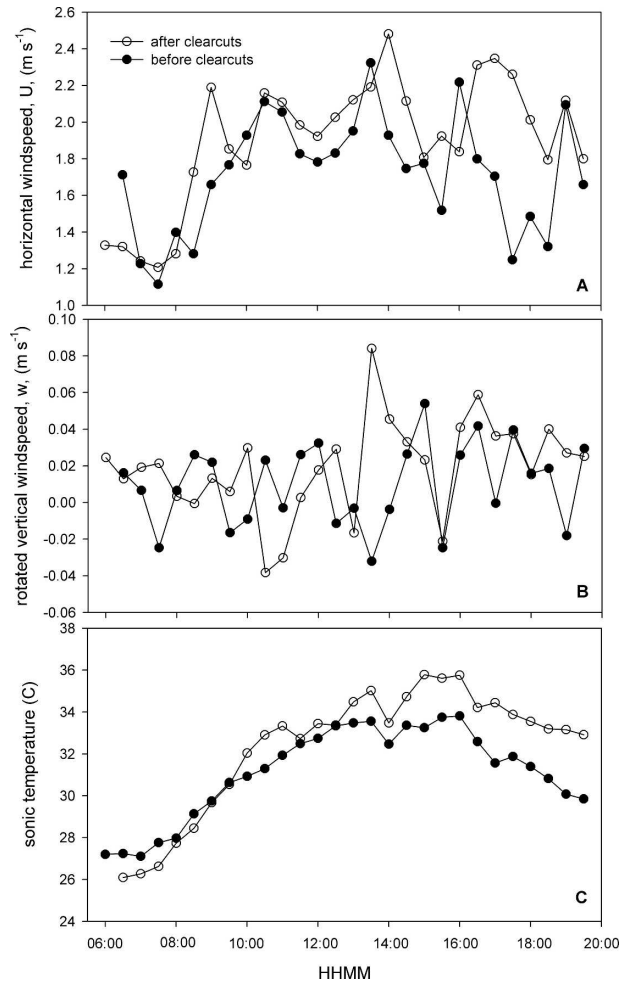


FIG. 6. Daytime median estimates of (a) U , (b) nonrotated w , and (c) T_s from the ACMF site. Data were collected in Jul 2000 and 2001 to contrast periods before and after the occurrence of the clear-cut near the Donaldson tower. The ACMF site was established 1-month before the formation of the clear-cut. The sample size for daytime data from Jul 2000 and 2001 were 266 and 489 30-min periods, respectively.

significant interactions with both $[CO_2]$ and the categorical variable cc suggest that this was not the case. We did, however, expect the sources of $[CO_2]$ within the clear-cuts after the harvest to be different from that of the intact forest. Significant interactions with both $[CO_2]$ and θ were also found in the data after the clear-cuts. This implies that the sources of variability for the significant interactions between $[CO_2]$ and θ on NEE_{max} were similar for periods before and after the clear-cut. To examine this further, we pooled together the pre- and post-clear-cut datasets and reanalyzed them; $U * w * [CO_2]$, $U * w * \theta$, and $U * T_a * \theta$ became insignificant (Table 2). Several new three-way effects became significant, all of which included T_a (Table 2),

TABLE 2. Results from an ANOVA general linear models of NEE_{max} and $\overline{w'T'_s}$ related to abiotic variables. A class variable cc was used to denote whether mass was being transported from the direction of the clear-cuts. Data from Jan 1999 to Jul 2000 were noted as “before clear-cuts,” data from Aug 2000 to Dec 2001 were noted as “after clear-cuts,” and the “entire dataset” was data from Jan 1999 to Dec 2001. Significant first-, second-, and third-order effects are listed ($p < 0.001$ and $\alpha = 0.05$), not significant (NS), and not applicable (—).

NEE_{max}			$\overline{w'T'_s}$		
Before clear-cuts	After clear-cuts	Entire dataset	Before clear-cuts	After clear-cuts	Entire dataset
$\theta * [CO_2] * cc$	$\theta * [CO_2] * cc$	$\theta * [CO_2] * cc$	—	—	—
$U * [CO_2] * \theta$	$U * [CO_2] * \theta$	$U * [CO_2] * \theta$	—	—	—
$U * [CO_2] * cc$	$U * [CO_2] * cc$	$U * [CO_2] * cc$	—	—	—
$w * [CO_2] * cc$	$w * [CO_2] * cc$	NS	—	—	—
$U * w * [CO_2]$	$U * w * [CO_2]$	NS	—	—	—
$U * w * \theta$	$U * w * \theta$	NS	$U * w * \theta$	$U * w * \theta$	$U * w * \theta$
$U * T_a * \theta$	$U * T_a * \theta$	NS	NS	NS	NS
NS	NS	$T_a * [CO_2] * cc$	NS	NS	NS
NS	NS	$T_a * \theta * cc$	NS	NS	NS
NS	NS	$T_a * \theta * [CO_2]$	NS	NS	NS
NS	NS	$T_a * w * U$	NS	NS	NS
$cc * \theta$	$cc * \theta$	$cc * \theta$	NS	NS	NS
NS	$cc * [CO_2]$	NS	—	—	—
NS	$U * [CO_2]$	NS	—	—	—
NS	$T_a * [CO_2]$	$T_a * [CO_2]$	—	—	—
NS	NS	$T_a * \theta$	NS	NS	NS
NS	NS	$T_a * U$	$T_a * U$	$T_a * U$	$T_a * U$
NS	NS	$T_a * cc$	NS	NS	NS
NS	NS	NS	$U * \theta$	$U * \theta$	$U * \theta$
NS	NS	NS	NS	$U * cc$	$U * cc$
NS	NS	NS	$U * w$	$U * w$	$U * w$
NS	NS	NS	$w * T_a$	$w * T_a$	$w * T_a$
NS	NS	NS	NS	$w * \theta$	$w * \theta$
NS	NS	NS	NS	$w * cc$	$w * cc$
θ	θ	θ	θ	θ	θ
NS	T_a	T_a	T_a	T_a	T_a
NS	NS	NS	w	w	w
NS	NS	NS	U	U	U
NS	NS	NS	cc	cc	cc
NS	NS	[CO ₂]	—	—	—

and most included some measure of wind direction and [CO₂]. Similarly, several two-way effects became significant—all of which included T_a and either some measure of wind direction or [CO₂].

The interaction between buoyancy flux and $U * w * \theta$ before the clear-cut was significant. After the clear-cuts, other two-way interactions became significant (Table 2).

Differences at the tower in θ before and after the clear-cuts were visually evident in wind roses (Fig. 7). Before the clear-cuts, the potential source areas were primarily from wind vectors between 30° and 60° from the tower (Figs. 7a and 7b). After the clear-cuts, the source areas became more general with a notable reduction around 45° (Figs. 7c and 7d). Median trends of temperature followed the same diurnal pattern before and after the clear-cuts (Fig. 8a); although after the clear-cuts, T_a was warmer before 0800 and cooler after 1830 LT. Median trends of U also followed a similar

diurnal pattern before and after the clear-cuts, though the trends diverged after 1830 LT (Fig. 8b). Median trends of w were always positive and increased after the clear-cut from 0600 to 1400 LT (Fig. 9a). The accuracy of the sonic is $\pm 0.005 \text{ m s}^{-1}$. During morning hours before the clear-cut, w was not significantly different from 0. Median diurnal time series of NEE_{max} were lower between 1200 and 1730 LT after the clear-cut (Fig. 10b). Median diurnal [CO₂] followed a similar pattern before and after the clear-cut, but with significantly higher concentrations of $\sim 50\text{--}60 \mu\text{mol CO}_2 \text{ mol}^{-1}$ afterward (Fig. 9b). Integrating the uptake across the daytime hours resulted in an $\sim 16.2\%$ loss in NEE_{max} after the clear-cut.

Differences in mean quantities of the integrated cospectra before and after the clear-cut were not significantly different among similar averaging times (Fig. 11a), but longer averaging times ($>30 \text{ min}$) contributed additional variability in NEE after the clear-cut (Figs.

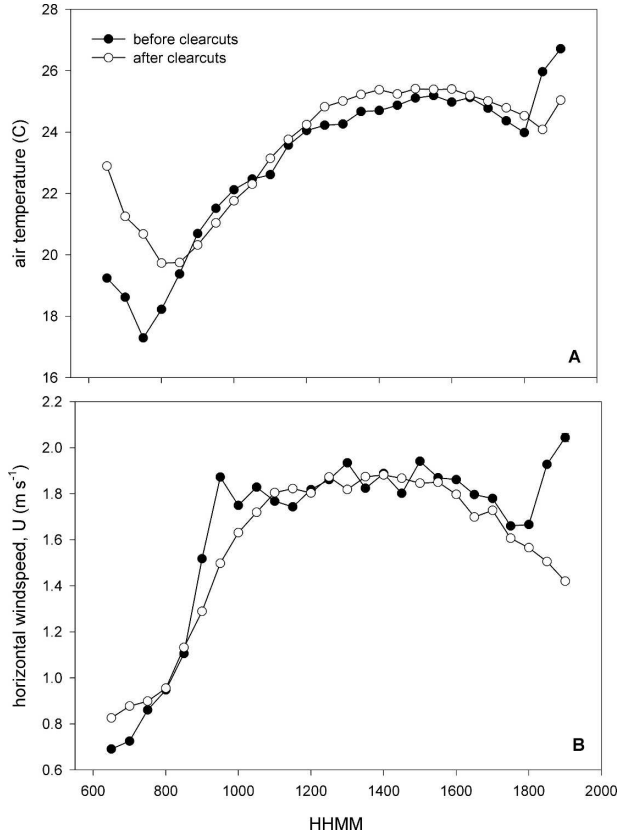


FIG. 8. Daytime median estimates of (a) T_a and (b) U before and after the occurrence of clear-cut patches in the source area of the Donaldson tract flux tower. Error bars are ± 1 SE.

thermal layers of the nocturnal boundary layer (NBL; Smith and Rutan 2003; Rosenberg et al. 1983; Mannoji 1995). In this scenario, the morning breakup of the NBL and the development of the CBL, and then the evening formation of the NBL were both delayed by 30 min after the clear-cut (Fig. 8). The large difference between the forest and clear-cut midmorning effective surface temperatures ($\sim 10^\circ\text{C}$) increased during summer months (data not shown), suggesting that much of the surface heating in the clear-cut was used to generate local convective motions. The development of local convective circulations was independently observed from the clear-cut areas after sufficient surface heating occurred (Leclerc et al. 2003).

The Donaldson site is located in one of the most micrometeorologically ideal forested ecosystems in the AmeriFlux network (i.e., uniform surface homogeneity, short roughness lengths, even-aged trees, and large fetch; <http://public.ornl.gov/ameriflux>). We expected the above-canopy CO_2 source strength to be uniform regardless of direction. Surprisingly, the significant interactions of $\theta * [\text{CO}_2] * \text{cc}$, $U * [\text{CO}_2] * \theta$, and $U *$

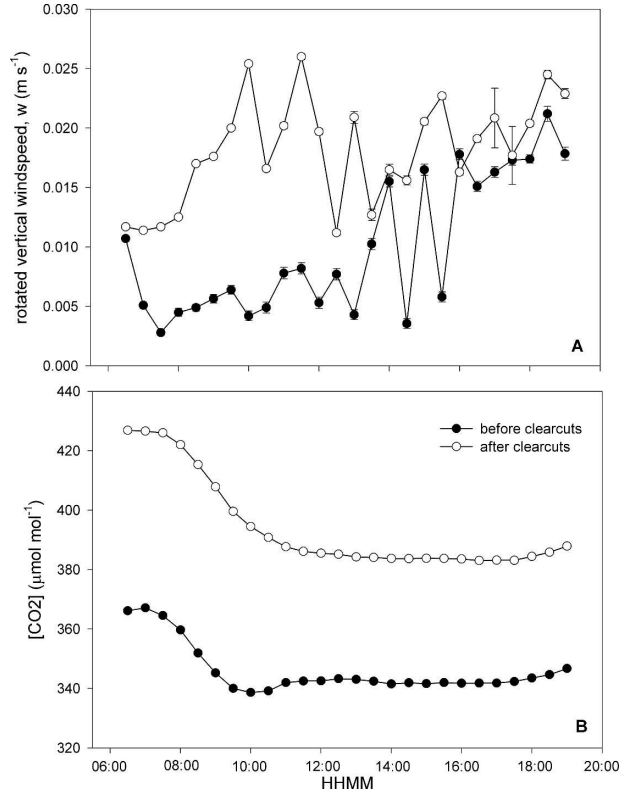


FIG. 9. Daytime median estimates of (a) rotated w and (b) CO_2 concentration before and after the occurrence of clear-cut patches in the source area of the Donaldson tract flux tower. Error bars are ± 1 SE.

$[\text{CO}_2] * \text{cc}$ suggest that this was not the case for NEE either before or after the clear-cuts and that the CO_2 source strength differed with wind direction even before the clear-cuts. This implies that probably all forested sites, however homogeneous in appearance have spatially heterogeneous source strengths with the potential to affect flux measurements and model results.

Convective circulations formed by the clear-cut area changed the patterns of wind direction over the tower site from those typically observed before the advent of the clear-cut (Fig. 7). The subsidence of these circulations likely occurred beyond the location of the tower, changing the overall CO_2 source area. While the exact location of this subsidence was unknown, it was, in part, dependent on the direction of surface winds in the convective boundary layer, and changed the direction of horizontal winds and source areas measured at the tower site. We interpret the positive vertical wind velocities (Fig. 9a) from 0600 to 1400 LT as the subsidence of convective cells into the forest at a location other than the area immediately surrounding the tower. The subsidence into the forest, in turn, caused almost con-

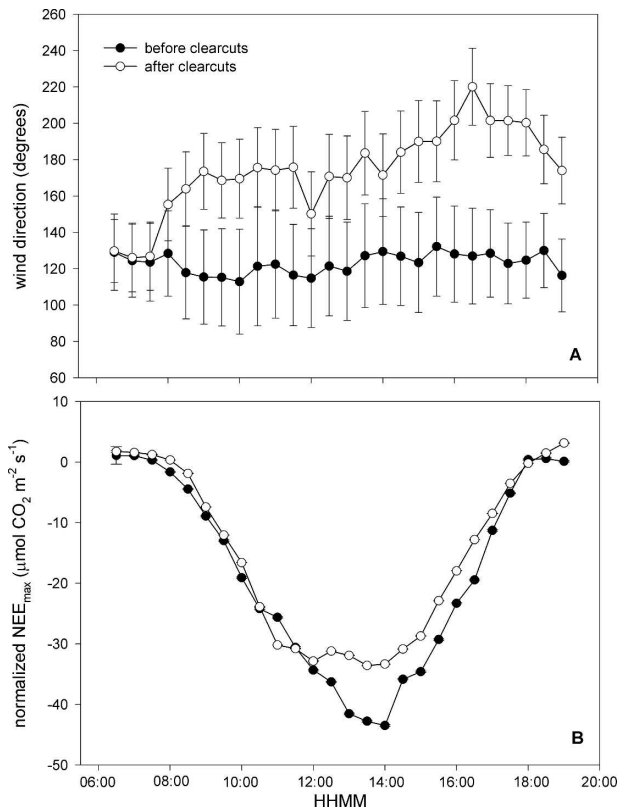


FIG. 10. Daytime median estimates of (a) wind direction and (b) NEE_{max} before and after the occurrence of the clear-cut in the source area of the Donaldson tract flux tower. Error bars are (a) ± 1 SD, and (b) ± 1 SE.

tinual positive vertical wind velocities that brought higher CO_2 from the clear-cuts. We would expect CO_2 to be higher in the clear-cut areas because logging debris was piled and left on site and planting preparation during the spring of 2001 included soil tillage (bedding), both of which suppressed regrowth. High CO_2 release from recent clear-cuts in this area is typical for about the first 3 yr after tree removal (Clark et al. 2004). The high nighttime CO_2 (data not shown) was not fully dissipated until ~ 1000 LT, so that additional CO_2 from below the canopy likely enriched the vertical fluxes of CO_2 measured at the sonic anemometer. Evidence that supports clear-cut-induced changes in local circulations affecting NEE_{max} are apparent in (i) the different significant three-way effects on NEE_{max} from before and after the clear-cuts (Table 2), (ii) the additional variability in low-frequency turbulence apparent through the integration of cospectra (Fig. 11; Sakai et al. 2001; Berger et al. 2001), and (iii) the different, significant two- and three-way effects on $\overline{w'T'_s}$ from before and after the clear-cuts, which were independent of the CO_2 source strength (Table 2).

The reduction in NEE_{max} following the clear-cut may be associated with long-term drought effects not accounted for by normalizing the VPD response on NEE (Rathgeber et al. 2003; Lagergren and Lindroth 2002). The decline in afternoon NEE_{max} after the clearcut (Fig. 10) was concurrent with the afternoon stomatal closure seen at the leaf level caused by this drought (T. A. Martin and G. Starr 2005, unpublished manuscript). The water table was often 2–4 m deep in these soils during 1999–2001, which is deeper than in normal precipitation years, but it is still likely that canopy trees had root access to the water table. Because the mean trends of the VPD were removed for every discrete 2-month period, and NEE_{max} and $\overline{w'T'_s}$ (after the clear-cut) were significantly different against turbulent variables other than T_s , we consider any additional effects resulting from a longer-term VPD response as being secondary (e.g., among years).

The clear-cut-induced changes in the microclimate and turbulent structure were unanticipated. The clear-cuts were located at a minimal distance of ~ 750 m, generally thought to be outside the source area of the flux tower. Our results suggest, however, that source area and strength were altered by the clear-cuts. Increased variability in the ogives and integral statistics after the clear-cut (Fig. 11) were likely due to the additional influence of nonstationarity. Often, ogives are used to determine the appropriate averaging time that incorporates all of the motions that transfer the scalar in question (Oncley et al. 1990). Lengthening the averaging time beyond 30 min did not contribute to any additional NEE , although conditions after the clear-cut promoted increased variability. A primary assumption of eddy covariance is consistent turbulence characteristics (i.e., stationarity) within the flux field over the averaging period. Longer averaging periods potentially increase the propensity of variable turbulent structures that can introduce additional uncertainties in the flux estimate. But, in this case, the creation of localized convective cells by the clear-cut area also increased uncertainties in flux estimates caused by variable turbulent structures. There are no accepted criteria or established threshold values that could determine acceptable limits of stationarity. Instead, it is up to individual sites to determine appropriate limits, even at apparently ideal sites. All flux sites should periodically examine the influences of low-frequency turbulence on measured fluxes (ogive analysis) in conjunction with integral turbulent statistics to assess data quality and the associated uncertainties. This is particularly true at sites with strong surface heating and patchiness in surface characteristics within the ecosystem, and those in areas of changing land use.

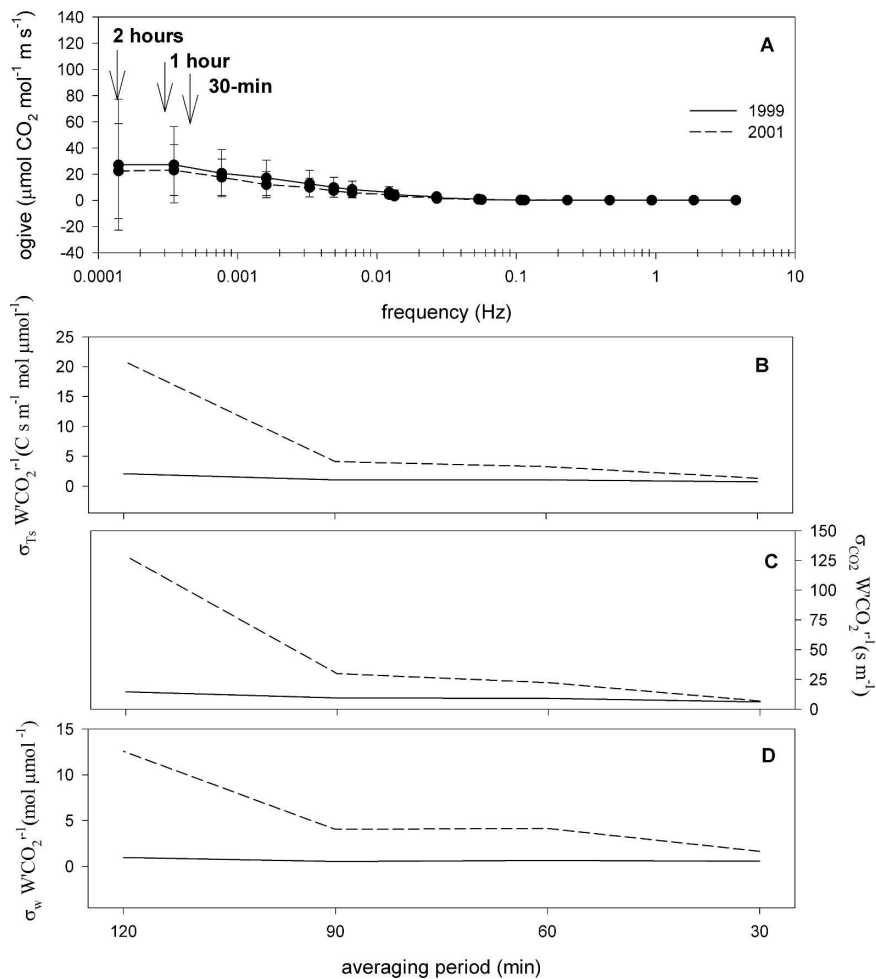


FIG. 11. (a) Daytime-integrated cospectra (ogives) and (b)–(d) integral turbulence statistics with different averaging periods for the Florida midrotation *P. elliottii* site. Before clear cutting (1999) data are from 21–24, 27–29 Apr, and 2–4, 30–31 May, and after clear cutting (2001) data are from 26–30 Apr, and 1–4 May. Cospectra were median absolute values, and error bars are ± 1 SD.

Acknowledgments. This work was supported, in part, by the U.S. Department of Energy Office of Science Contract DE-FC03-90ER61010 as part of National Institute for Global and Environmental Change. We thank L. Mahrt, K. Clark, M. Kurpius, L. Hipps, M. Leclerc, and A. Karipot for discussions concerning earlier drafts of this paper. The authors also thank R. Clement and S. Richmond for programming assistance, and the anonymous reviewers for their careful and thoughtful comments.

REFERENCES

- Alley, W. M., 1984: The Palmer drought severity index: Limitations and assumptions. *J. Climate Appl. Meteor.*, **23**, 1100–1109.
- Berger, B. W., K. J. Davis, C. X. Yi, P. S. Bakwin, and C. L. Zhao, 2001: Long-term carbon dioxide fluxes from a very tall tower in a northern forest: Flux measurement methodology. *J. Atmos. Oceanic Technol.*, **18**, 529–542.
- Black, T. A., and Coauthors, 2000: Increased carbon sequestration by a boreal deciduous forest in years with a warm spring. *Geophys. Res. Lett.*, **27**, 1271–1274.
- Buck, A., 1981: New equations for computing vapor pressure and enhancement factor. *J. Appl. Meteor.*, **20**, 1527–1532.
- Clark, K. L., H. L. Gholz, J. B. Moncrieff, F. Croppley, and H. W. Loescher, 1999: Environmental controls over net exchanges of carbon dioxide from contrasting Florida ecosystems. *Ecol. Appl.*, **9**, 936–948.
- , —, and M. S. Castro, 2004: Carbon dynamics along a chronosequence of slash pine plantations in north Florida. *Ecol. Appl.*, **14**, 1154–1171.
- Foken, T., and B. Wichura, 1996: Tools for quality assessment of surface-based flux measurements. *Agric. For. Meteorol.*, **78**, 83–105.
- Gash, J. H. C., and A. J. Dolman, 2003: Sonic anemometer (co)sine response and flux measurement. I. The potential for

- (co)sine error to affect sonic anemometer-based flux measurements. *Agric. For. Meteorol.*, **119**, 195–207.
- Gholz, H. L., and K. L. Clark, 2002: Energy exchange across a chronosequence of slash pine forests in Florida. *Agric. For. Meteorol.*, **112**, 87–102.
- Goulden, M. L., J. W. Munger, S. M. Fan, B. C. Daube, and S. C. Wofsy, 1996: Measurements of carbon sequestration by long-term eddy covariance: Methods and a critical evaluation of accuracy. *Global Change Biol.*, **3**, 169–182.
- Greco, S., and D. D. Baldocchi, 1996: Seasonal variations of CO₂ and water vapour exchange rates over a temperate deciduous forest. *Global Change Biol.*, **3**, 183–197.
- Jarvis, P. G., 1976: The interpretation of the variations in leaf water potential and stomatal conductance found in canopies in the field. *Philos. Trans. Roy. Soc. London*, **273B**, 593–610.
- , J. M. Massheder, S. E. Hale, J. B. Moncrieff, M. Rayment, and S. L. Scott, 1997: Seasonal variation of carbon dioxide, water vapor, and energy exchanges of a boreal black spruce forest. *J. Geophys. Res.*, **102**, 28 953–28 966.
- Kaimal, J. C., and J. E. Gaynor, 1991: Another look at sonic thermometry. *Bound.-Layer Meteorol.*, **56**, 401–410.
- Kanda, M., A. Inagaki, M. O. Letzel, S. Raasch, and T. Watanabe, 2004: LES study of the energy imbalance problem with eddy covariance fluxes. *Bound.-Layer Meteorol.*, **110**, 381–404.
- Karl, T. R., and R. W. Knight, 1985: *Atlas of Monthly Palmer Hydrological Drought Indices (1931–1983) for the Contiguous United States*. Historical Climatology Series 3–9, National Climate Data Center, 319 pp.
- Lagergren, F., and A. Lindroth, 2002: Transpiration response to soil moisture in pine and spruce trees in Sweden. *Agric. For. Meteorol.*, **112**, 67–85.
- Leclerc, M. Y., A. Karipot, T. Prabha, G. Allwine, B. Lamb, and H. L. Gholz, 2003: Impact of non-local advection on flux footprints over a tall forest canopy: A tracer flux experiment. *Agric. For. Meteorol.*, **115**, 17–34.
- Letzel, M. O., and S. Raasch, 2003: Large-eddy simulation of thermally induced oscillations in the convective boundary layer. *J. Atmos. Sci.*, **60**, 2328–2341.
- Loescher, H. W., and Coauthors, 2005a: Comparison of temperature and wind statistics in contrasting environments among different sonic anemometer-thermometers. *Agric. For. Meteorol.*, **133**, 119–139.
- , H. L. Gholz, J. M. Jacobs, and S. F. Oberbauer, 2005b: Energy dynamics and modeled evapotranspiration from a wet tropical forest in Costa Rica. *J. Hydrol.*, **315**, 274–294.
- , B. E. Law, L. Mahrt, D. Hollinger, J. L. Campbell, and S. C. Wofsy, 2006: Addressing uncertainties in carbon estimates using the eddy covariance technique. *J. Geophys. Res.*, in press.
- Livingston, N. J., and T. A. Black, 1987: Stomatal characteristics and transpiration of three species of conifer seedlings planted on a high elevation south-facing clear-cut. *Can. J. For. Res.*, **17**, 1273–1282.
- Mannaji, N., 1995: An explicit cloud predicting scheme implemented in the Florida State University Global Spectral Model and its impact. *J. Meteor. Soc. Japan*, **73**, 993–1009.
- Martin, T. A., and Coauthors, 1997: Crown conductance and tree and stand transpiration in a second-growth *Abies amabilis* forest. *Can. J. For. Res.*, **27**, 797–808.
- Moncrieff, J. B., and Coauthors, 1997: A system to measure surface fluxes of momentum, sensible heat, water vapour and carbon dioxide. *J. Hydrol.*, **189**, 589–611.
- Moore, C. J., 1986: Frequency response corrections for eddy correlation systems. *Bound.-Layer Meteorol.*, **37**, 17–35.
- Oke, T. R., 1978: *Boundary Layer Climates*. Routledge Press, 434 pp.
- Oncley, S. P., J. A. Businger, E. C. Itsweire, C. A. Friehe, J. C. LaRue, and S. S. Chang, 1990: Surface layer profiles and turbulence measurements over uniform land under near-neutral conditions. Preprints, *9th Symp. on Boundary Layer and Turbulence*, Roskilde, Denmark, Amer. Meteor. Soc., 237–240.
- Palmer, W. C., 1965: Meteorological drought. U.S. Department of Commerce Weather Bureau Research Paper 45, 58 pp.
- Paw U, K. T., D. D. Baldocchi, T. P. Meyers, and K. B. Wilson, 2000: Correction of eddy-covariance measurements incorporating both advective effects and density fluxes. *Bound.-Layer Meteorol.*, **97**, 487–511.
- Pilegaard, K., P. Hummelshoj, N. O. Jensen, and Z. Chen, 2001: Two years of continuous CO₂ eddy-flux measurements over a Danish beech forest. *Agric. For. Meteorol.*, **107**, 29–41.
- Rathgeber, C., A. Nicault, J. O. Kaplan, and J. Guiot, 2003: Using a biogeochemistry model in simulating forests productivity responses to climatic change and [CO₂] increase: Example of *Pinus halepensis* in Provence (south-east France). *Ecol. Modell.*, **166**, 239–255.
- Rosenberg, N. J., B. L. Blad, and S. B. Verma, 1983: *Microclimate: The Biological Environment*. John Wiley and Sons, 495 pp.
- Running, S. W., D. D. Baldocchi, D. P. Turner, S. T. Gower, P. S. Bakwin, and K. A. Hibbard, 1999: A global terrestrial monitoring network integrating tower fluxes, flask sampling, ecosystem modeling and EOS satellite data. *Remote Sens. Environ.*, **70**, 108–127.
- Sakai, R. K., D. R. Fitzjarrald, and K. E. Moore, 2001: Importance of low-frequency contributions to eddy fluxes observed over rough surfaces. *J. Appl. Meteorol.*, **40**, 2178–2192.
- Schuepp, P. H., M. Y. Leclerc, J. I. Macpherson, and R. L. Desjardins, 1990: Footprint prediction of scalar fluxes from analytical solutions of the diffusion equation. *Bound.-Layer Meteorol.*, **50**, 355–373.
- Smith, G. L., and D. A. Rutan, 2003: The diurnal cycle of outgoing longwave radiation from earth radiation budget experiment measurements. *J. Atmos. Sci.*, **60**, 1529–1542.
- Song, C., C. E. Woodcock, K. C. Seto, M. P. Lenney, and S. A. Macomber, 2001: Classification and change detection using Landsat TM data: When and how to correct atmospheric effects. *Remote Sens. Environ.*, **75**, 230–244.
- Sun, J., R. Desjardins, L. Mahrt, and I. MacPherson, 1998: Transport of carbon dioxide, water vapor and ozone by turbulence and local circulations. *J. Geophys. Res.*, **103**, 25 873–25 885.
- Synder, W. C., Z. Wan, Y. Zhang, and Y. Z. Feng, 1998: Classification-based emissivity for land surface temperature measurement from space. *Int. J. Remote Sens.*, **19**, 2753–2774.
- Teskey, R. O., H. L. Gholz, and W. P. Cropper Jr., 1994: Influence of climate and fertilization on net photosynthesis of mature slash pine. *Tree Phys.*, **14**, 1215–1227.
- Valentini, R., P. DeAngelis, G. Matteucci, R. Monaco, S. Dore, and G. E. S. Mugnozza, 1996: Seasonal net carbon dioxide exchange of a beech forest with the atmosphere. *Global Change Biol.*, **2**, 199–207.
- Wilczak, J. M., S. P. Oncley, and S. A. Stage, 2001: Sonic anemometer tilt correction algorithms. *Bound.-Layer Meteorol.*, **99**, 127–150.
- Wright, I. R., J. H. C. Gash, H. R. da Rocha, and J. M. Roberts, 1996: Modelling surface conductance for Amazonian pasture and forest. *Amazonian Deforestation and Climate*. J. H. C. Gash et al., Eds., John Wiley and Sons, 437–458.